First-Principles Study of Pressure-Induced Amorphization of Fe_2SiO_4 Fayalite

Masaaki Misawa[1,2] and Fuyuki Shimojo[2]*

((Optional Dedication))
Dr. M. Misawa
[1]Graduate School of Natural Science and Technology, Okayama University, Okayama 700-8530, Japan,
[2]Faculty of Science and Engineering, Kyushu Sangyo University, Fukuoka 813-8503, Japan
E-mail: misawa@okayama-u.ac.jp

Prof. F. Shimojo
[3]Department of Physics, Kumamoto University, Kumamoto 860-8555, Japan

Keywords: iron silicate, amorphous structure, molecular dynamics, density functional theory

Abstract

Fayalite (Fe_2SiO_4), which is an end-member of the olivine series ($(Fe_xMg_{1-x})_2SiO_4$), undergoes a crystal-to-amorphous transformation under high-pressure at room temperature conditions. This pressure-induced amorphized fayalite has an interesting feature: it exhibits antiferromagnetism at low temperature regardless of its non-crystalline structure. In spite of this unique property, first-principles investigations of pressure-induced amorphized fayalite have not yet been carried out. In this study, to clarify the energetic and structural properties of pressure-induced amorphized fayalite, we performed first-principles molecular dynamics simulations of the compression and decompression processes of fayalite in the pressure range 0-120 GPa. The energetic and structural properties were also compared with those of well-equilibrated melt-quenched amorphous Fe_2SiO_4. Based on structural analysis, it was confirmed that not only six-fold but also five-fold coordinated silicon atoms exist in the amorphous-like structure under high-pressure. Additionally, it was found that the silicon atoms play the role of network-former in the amorphous-like phase under high pressure, but change to a network-modifier role after release to ambient conditions. Moreover, it was found that the obtained amorphous-like phase has a partially ordered structure. It is inferred that the partially ordered structure likely enables the pressure-amorphized fayalite to exhibit antiferromagnetism.

1. Introduction

Fayalite (Fe_2SiO_4), which is an end member of the olivine series ($(Fe_xMg_{1-x})_2SiO_4$), is the important component in the upper mantle of the Earth. In the crystalline fayalite, Fe and Si ions are located on six-fold octahedral and four-fold tetrahedral sites, respectively, in a hexagonal close-packed framework of O ions. In this structure, the SiO_4 tetrahedrons are isolated and FeO_6 octahedrons connect to each other via edge sharing. Because of the electronic spin polarization of the d-electrons in Fe ions, fayalite exhibits intrinsic antiferromagnetism below the Néel temperature (~ 65 K). For decades, the structural, magnetic and elastic properties of fayalite under high-temperature and high-pressure conditions have been investigated experimentally for crystalline,[1] molten,[2] and liquid[3] phases because of its importance in geoscience.

In 1990, it was reported that the crystalline fayalite undergoes a crystal-to-amorphous transformation under compression to ~40 GPa at room temperature.[4] While this pressure-induced amorphization can also be observed in other olivine minerals, the transition pressure of fayalite is the lowest.[5] Furthermore, it was found that the pressure-amorphized phase also exhibits antiferromagnetism with a Néel temperature similar to that of the crystalline phase in spite of its non-crystalline structure.[6] Because of its unique nature, elucidating the electronic and structural properties of crystalline and pressure-amorphized fayalite is very important, not only for geochemistry but also materials science. From *in-situ* X-ray diffraction and the infrared measurements, it has been inferred that the pressure-induced amorphization is triggered by an increase in the coordination number of Si atoms. Specifically, tetrahedral SiO_4 units in the crystalline phase are expected to be destabilized due to the high pressure, and transform into octahedral SiO_6 or pyramidal SiO_5 units.[4a]

However, some questions remain: the ratio of the octahedral SiO_6 and pyramidal SiO_5 units; the properties of the network structure in the amorphous phase; and why pressure-induced amorphized fayalite can exhibit antiferromagnetism in spite of its non-crystalline structure. In

addition, the energetic properties of the amorphous phase have not been fully elucidated. Furthermore, while computational investigations have been successful in studying the structural, electronic, magnetic and optical properties of crystalline,[7] liquid[8], and molten fayalite under high-pressure conditions, the properties of the pressure-amorphized phase have not yet been studied theoretically. Considering these points, we performed first-principles molecular dynamics (FPMD) simulations of the compression and decompression processes of fayalite to elucidate the energetic and structural properties of pressure-induced amorphized fayalite.

2. Computational Details

The FPMD simulations of fayalite in this study were all performed using QXMD code.[9] The electronic states were calculated based on the projector augmented-wave method,[10] within the framework of density functional theory (DFT). The Perdew-Burke-Ernzerhof (PBE) generalized gradient approximation was used for the exchange-correlation energy.[11] A plane-wave basis set with cutoff energies of 30 and 300 Ry was employed for the pseudo-wave functions and pseudo-charge density, respectively. Projector functions were generated for the 3d4s4p states of Fe, 2s2p states of Si, and 2s2p states of O atoms. To correctly represent the electronic states in localized d-orbitals of Fe, the DFT+U method with effective parameter for the Coulomb interaction U_{eff} = 4.0 eV was used.[12] Collinear spin-polarization was taken into account to reproduce the thermodynamic behaviors of iron oxide based compounds correctly.[13] Antiferromagnetic alignment of Fe atoms was employed as the initial magnetic state based on the theoretical prediction.[14] A local magnetic moment for Fe of $|M_{\mathrm{s}}|$ = 3.9 μ_{B}/atom was obtained by static calculations, showing excellent agreement with previous DFT+U calculations.[14-15] Note that the magnetic moment of the whole system maintained a value of zero during the compression and decompression MDs. The absolute value of the local magnetic moment of Fe decreased slightly with increasing pressure, but was almost recovered after decompression (Fig. S1). Only the Γ-point was used for Brillouin zone sampling. A

supercell consisting of 168 atoms ($Fe_{48}Si_{24}O_{96}$), which corresponds to 3×1×2 of the unit cell of crystalline fayalite, was employed as the simulation system. Periodic boundary conditions were employed in all directions to simulate bulk material. The equations of motion were solved via an explicit reversible integrator,[16] under an isothermal-isobaric ensemble.[17] The temperature of 300 K was maintained during the FPMD simulations.

Under experimental conditions, pressure-induced amorphization is observed at 42.1 GPa.[4a] However, the timescale required for this condition would be much too long to observe directly in the FPMD method. Therefore, in our FPMD simulations, the crystalline fayalite was first compressed from ambient pressure (0 GPa) up to 120 GPa to achieve the pressure-induced structural transformation at room temperature within a computationally feasible timescale. The pressure was increased and decreased step-by-step by 10 GPa every 2.4 ps in the compression and decompression processes, respectively. For each compression and decompression step, the latter half of the time (1.2 ps, 1000 steps) was used to collect all physical quantities, e.g. the average values of potential energy, specific volume, coordination number and pair distribution functions. The total simulations time was 31.2 ps (15.6 ps compression + 15.6 ps decompression) with a time step of 1.2 fs.

In addition, two types of amorphous Fe_2SiO_4 were also made by melt-quenching (MQ) processes to compare their energetic and structural properties with the compression and decompression sample, as described later. The first one was melted at 3000 K at ambient pressure (0 GPa), then quenched to room temperature. The second one was first melted at 4000 K under 120 GPa pressure, then quenched to room temperature, and subsequently decompressed to 0 GPa. Note that further compression was performed up to 200 GPa, but the Si atoms did not change their coordination geometries above 120 GPa (see Figure S2 in the supporting information). Based on this result, the decompression simulation was started from 120 GPa. The simulation time for each process was 1.8 ps. In order to calculate the average

energy, volume, coordination number and radial distribution functions of these MQ samples, additional MD simulations were carried out 1.2 ps after release to ambient conditions.

3. Results and Discussion

3.1. Energetic Properties

First, the energetic properties of fayalite during the compression and decompression processes were investigated. **Figure 1**a shows the average potential energies as a function of pressure. The potential energy of crystalline fayalite under ambient conditions was set to zero. It appears that at least two phases are present because the lines for compression and decompression processes are clearly separated between 0 and 100 GPa. The two lines are almost indistinguishable at 110 and 120 GPa. Hence, it is considered that the crystalline phase was transformed to some other phase upon compression from 100 to 110 GPa. The potential energies of the crystalline phase at pressures up to 30 GPa are lower than that of the transformed phase at 0 GPa as shown by the gray dotted line. This means that the crystalline fayalite requires more than 30 GPa to achieve the pressure-induced structural transformation, energetically. This feature is consistent with a previously reported experimental observation that the crystallographic space group of fayalite was not changed by compression up to 31 GPa.[18]

Figure 1b shows the average potential energy as a function of the average specific volume during the compression and decompression processes. The average volume of crystalline fayalite in the FPMD simulation at 0 GPa was set to 1. Using data from 0 to 100 GPa for compression and from 120 to 0 GPa for decompression processes, least squares fitting curves to the third-order Birch-Murnaghan equation of state (BMEoS) were generated (solid red and dashed blue lines, respectively). Additionally, the BMEoS curve of crystalline fayalite estimated based on the experimentally determined isothermal bulk modulus at ambient conditions based on an *in situ* X-ray diffraction experiment is also shown as a green dash-dotted curve.[19] For this curve, the experimentally measured volume of single crystal fayalite at

ambient conditions was set to 1. As we can see, the fitting curve for the compression data shows good agreement with the experimental BMEoS curve for crystalline fayalite, indicating that the crystalline phase was maintained up to 100 GPa in the FPMD simulations. On the other hand, after being compressed to 110 GPa, the energy-volume plots fall outside the experimental BMEoS curve and locate on the decompression curve. The decompression and compression curves cross at a specific volume of 0.78, which corresponds to between 40 and 50 GPa of compression. This energetic equivalence is consistent with the experimental observation that the pressure-induced amorphization occurred above 40 GPa under room temperature conditions.[4a]

For further information related to the energetic properties, the partial electronic density of states (PDOSs) during the compression and decompression processes were calculated (Figure S3). The band gap energies of crystalline fayalite under pressure shown in the figures are consistent with a previously reported first-principles investigation.[20]

It was confirmed that the energetic properties obtained by our FPMD simulations are reasonable enough for discussion of the experimentally observed pressure-induced amorphization of fayalite; however, the equilibration time scale in the MD simulations could be insufficient. To test whether the equilibration time was long enough, amorphous Fe_2SiO_4 was made by a melt-quenching (MQ) process at 0 GPa. Additionally, to mimic the equilibration at high pressure, an MQ sample was made also at 120 GPa, then decompressed to 0 GPa. The energetic properties of the MQ samples made at 0 and 120 GPa are indicated as green squares and orange circles in Figs. 1a and b, respectively. As shown in Fig. 1b, the densities of the MQ samples are lower than that of the crystalline phase at 0 GPa, but the potential energies are almost the same as for the blue data point at 0 GPa. From these results, it is expected that the equilibration time for the compression and decompression processes is insufficient, but the transformed phase obtained by the compression and decompression processes is energetically close to ordinary amorphous Fe_2SiO_4. Therefore, hereinafter, the transformed phase is referred

to as an "amorphous-like" phase in this paper. To test whether further structural changes can be observed for longer FPMD simulation, an extended FPMD simulation at 120 GPa and room temperature were performed up to 20 ps. To accelerate the simulation, the timestep Δt = 2.0 fs was employed in this simulation based on the energy conserving test (Figure S4). As a result of the extended simulation, it was found that observation of further structural changes at high pressure and room temperature conditions is quite difficult within the framework of FPMD method, because there were almost no changes in energetic and structural properties. Specifically, while the potential energy (Figures S5a and b) and non-diagonal components of the stress tensor (Figures S5c and d) have likely converged, its volume (Figure S5e) and coordination numbers of Fe and Si atoms (Figure S5f) remain unchanged over time. Therefore, it is considered that the structural changes observed in our simulations are close to the practical limit of FPMD method at room temperature condition. Note that the MQ sample made at high pressure is about 8.7% denser than that made at ambient pressure at 0 GPa. This result means that a permanent densification phenomenon occurred in the amorphous Fe_2SiO_4 system.

3.2. Pair Distribution Function

To study the structural changes of fayalite during the compression and decompression processes, partial pair distribution functions (PDF) for 0, 40, 80 and 120 GPa were calculated. **Figure 2**a shows PDFs for cation-anion pairs. The main peak positions in the PDFs for Fe-O and Si-O correlations correspond to their equilibrium interatomic bond distances. Those in the crystalline phase at 0 GPa are shown as a gray dotted line in Figure 2a. If the structural units are simply compressed, the peak positions will shift to the left side with increasing pressure. For the Fe-O correlation, the main peak position monotonically shifted to the left side with increasing pressure. After decompression, the peak position almost returned to the original position in the crystalline phase at 0 GPa. On the other hand, for the Si-O correlation, first the main peak position first shifted slightly to the left side up to 80 GPa, but then went back to the

original position at 120 GPa. This behavior indicates that the local coordination geometry of Si atoms changed during the phase transition. The peak position of the Si-O correlations was almost unchanged in the decompression process, except at 40 GPa. It is speculated that some changes in local geometry occurred around Si atoms at 40 GPa, whose details will be described in the next section.

The PDFs for anion-anion pairs are shown in Figure 2b. This O-O correlation could be loosely separated into two regions: the area from 2 to 4 Å and from 4 to 6 Å. The first region mainly consists of lengths between apexes in a structural unit, and the second one corresponds to the distances between apexes in two different structural units. These correlations broadened with the compression and decompression processes; however, the overall trend was conserved even after decompression of the amorphous-like phase.

The PDFs for cation-cation pairs, which characterize distances and arrangements between Fe-centered and silicon-centered structural units, are shown in Figure 2c. The Fe-Fe correlation was broadened by the compression and decompression processes, but still had a sharp peak at the right side of the first peak after decompression. This behavior suggests that some medium- or long-range order remained in the partial structure of Fe atoms, which may help to explain the antiferromagnetism in the pressure-amorphized fayalite at low temperature. The Si-Si correlations were almost unchanged up to 80 GPa, but a short-range correlation at less than 3.5 Å was generated with compression to 120 GPa. This corresponds to a connectivity change between SiO_x structural units. It is expected that the isolated SiO_x units in the ideal crystalline phase become joined together during the phase transition, and formed an Si-O network in the amorphous-like phase. The details of the network structure in the amorphous-like phase will be described in section 3.4. The Fe-Si correlation had two major peaks in the crystalline phase from 0 GPa to 80 GPa, but they merged into one peak at 120 GPa even after decompression. The two types of crystallographic sites for Fe atoms in the crystalline phase cause the existence of two major peaks in the Fe-Si correlation. The merged peak denotes that

the iron atoms located on the two crystallographic sites became indistinguishable due to the phase transition.

The PDFs for the MQ samples made at 0 and 120 GPa were also calculated and are shown in Fig. 2 as green and orange dashed curves, respectively. We can see that the local structures were relaxed during MQ at 120 GPa. Under ambient conditions, most of the PDFs show similar tendencies, but only the Fe-Fe correlations for MQ samples are distinctly different from the amorphous-like phase.

From the PDFs, it was found that the local coordination geometries and arrangement of structural units change during compression and decompression process. Furthermore, some degree of medium- or long-range order of Fe atoms remained in the amorphous-like phase. Based on these findings, the pressure dependence of the coordination numbers of cations and the amorphous-like structure will be discussed in the subsequent sections.

3.3. Coordination Number

To study changes in the local coordination geometry of cations during the compression and decompression processes, the average coordination numbers of iron and silicon atoms as a function of pressure are shown in **Figure 3**a. To calculate the coordination number, the cutoff distances for Fe-O and Si-O bonds are defined as 2.8 and 2.1 Å, respectively. Note that these criteria were decided based on the the saddle point in the PDFs for cation-anion correlations under ambient conditions, though the saddle point in the Fe-O correlation distribution became unclear under high-pressure conditions. For the compression process, all Fe and Si atoms maintained their original coordination numbers in the crystalline phase up to 30 GPa. Above 30 GPa, the coordination number of Fe began increasing earlier than that of Si, and reached 7.0 at 100 GPa. With further compression, the coordination number of both Fe and Si sharply increased, accompanied by the phase transition. From the previous experiments, it was anticipated that the increment in the coordination number of Si from four to six triggered the

pressure-induced amorphization.[4b] In our simulation, the average coordination number of Si became 5.7 during the phase transition. In the decompression process, the coordination number of Fe monotonically decreased and returned to nearly six at 0 GPa. On the other hand, the coordination number of Si first slightly decreased until 50 GPa first, then increased again to 5.7 at 40 GPa, and decreased again as the pressure approached 0 GPa. Eventually the average coordination number of Si atoms became 4.8 at 0 GPa. This result demonstrates that high-fold coordinated Si atoms remained in the amorphous-like phase even after releasing the pressure to ambient conditions. Such irreversible coordination changes for Si atoms are also reported for quenching processes of silica glass from high-pressure conditions.[21]

Figure 3b shows the distributions of four-, five- and six-fold coordinated Si atoms as a function of pressure in the decompression process. At 120 GPa, there are no four-fold coordinated Si atoms remaining, and two-thirds and one-thirds of the Si atoms are in six- and five-fold coordination geometries, respectively. The six-fold coordinated Si atoms decreased their coordination number with decreasing pressure until 50 GPa, but were reformed at 40 GPa, which is nearly the experimental pressure where the pressure-induced amorphization was observed. This behavior appears to be related to the peak shift of PDFs for Si-O correlation at 40 GPa shown in Figure 2c. At this condition, about 28% and 5% of the five-fold and four-fold coordinated Si atoms coexisted. With further decompression, the numbers of six- and four- fold coordinated Si atoms drastically decreased and increased until 0 GPa, respectively. Meanwhile, the distribution of five-fold coordinated Si atoms did not change much. Eventually the four-fold coordinated Si atoms became dominant at 0 GPa, which is consistent with the experimental prediction,[4b] but about the half of the Si atoms were still in high-fold coordination geometries.

The average coordination number and distribution of the coordination number of Si atoms for MQ samples made at 0 and 120 GPa were also calculated (green and orange symbols in Fig. 3, respectively). The coordination number of Fe atoms was not changed during the MQ process at 120 GPa, but became almost 5 after decompression to 0 GPa, while most of Fe atoms

exhibit six-fold coordination geometry in the amorphous-like phase. In the MQ sample made at 0 GPa, nearly half of the Fe atoms adopt five-fold coordination geometry. This difference in the local coordination geometry of Fe atoms results in a different arrangement of Fe atoms, which is also reflected in the pair distribution functions (see Fig. 2c). On the other hand, Si atoms in the MQ samples preferred four-fold coordination geometry under ambient conditions. The proportions of six- and five-fold coordinated Si atoms in the MQ samples were lower than in the amorphous-like phase at 0 GPa.

To conclude of this section, it was found that not only six-fold but also five-fold coordinated Si atoms exist in the amorphous-like phase. The six-fold coordinated Si atoms are dominant under high-pressure (~40 GPa) conditions, but are overtaken by four-fold coordinated Si atoms as the pressure nears 0 GPa.

3.4. Amorphous Structure

To further understand the structural properties of the amorphous-like phase, snapshots of the fayalite structure obtained by the FPMD simulations are displayed in **Figure 4**. Figures 4a-4c show the SiO_x polyhedrons in the crystalline and amorphous-like phases. As previously mentioned, Si atoms form SiO_4 tetrahedral units, and they are not connected with each other in the crystalline phase (Figure 4a). After the phase transition, the majority of the Si atoms changed into high-fold coordinated SiO_5 pyramidal or SiO_6 octahedral units as shown in Figure 3. At the same time, the SiO_x polyhedrons also changed their connectivity. At 40 GPa, all of them were connected to each other by corner or edge sharing, playing the role of network-former in the amorphous-like phase (Figure 4b). However, when the amorphous-like phase was decompressed to 0 GPa, some of the units become disconnected and separated into 9 fragments (Figure 4c). Therefore, it is considered that the Si atoms behave as a network-modifier rather than network-former under ambient conditions.

The atomic configurations of Fe and Si atoms in the amorphous-like phase are displayed as Figures 4d-4i. Based on the PDFs shown in Figure 2, it was expected that the medium- and long-range order of the Fe atoms might remain in the amorphous-like phase. The Fe and Si atoms seem to be fully disordered from the y-z plane view (Figure 4d), but not from the other view. For the z-x plane view, we can see a horizontal stripe pattern consisting of Fe and Si atoms (red highlighted in Figure 4e). Furthermore, a hexagonal orientation is clearly seen in the x-y plane view, which is not seen in the crystalline phase (red highlighted in Figure 4f). After decompression to 0 GPa, the atomic configurations are disordered more than at 40 GPa, but still show partial order (red highlighted in Figure 4g-i).

Finally, structure factors for the crystalline and amorphous-like phases are shown in **Figure 5**. We can see that the crystallinity was decreased substantially by the phase transition, but the medium- and long-range order still remained in the amorphous-like phase, especially at 40 GPa. Based on these results, it is considered that pressure-induced amorphized fayalite has a partially ordered or crystallized structure. The obtained average atomic positions and cell lengths during the decompression process at 120, 40 and 0 GPa are available as a supporting information file (ConfigS1-S3.pdb).

4. Summary

In summary, we performed FPMD simulations of the compression and decompression processes of fayalite to investigate the energetic and structural properties of pressure-induced amorphized fayalite. The energetic properties of the crystalline and amorphous-like phases of fayalite obtained from the simulations were reasonable and consistent with the experimental observations. Then, the density and potential energy of the amorphous-like phase were compared with those of highly disordered amorphous Fe_2SiO_4 samples made by MQ processes at 120 and 0 GPa. The amorphous-like phase was much denser than the MQ samples at 0 GPa, suggesting that the equilibration time for the compression and decompression processes was

insufficient. On the other hand, the potential energies of the amorphous-like phase and such MQ samples were very close. Additionally, there are some structural features common to the amorphous-like phase and the MQ sample made at high pressure. The local coordination geometries of Fe and Si atoms were investigated, and it was found that six- and five-fold coordinated Si atoms exist in the amorphous-like phase. These high-fold coordinated Si atoms still exist after decompression at 0 GPa while the majority of the Si atoms return to four-fold coordination. The SiO_x structural units connect with each other and play the role of the network-former in the amorphous-like phase under high pressure, but change to a network-modifier role after quenching. Moreover, it is expected that the partially ordered or crystallized structures exist in the amorphous-like phase, resulting in the antiferromagnetic behavior of the amorphous material.

Acknowledgements

This study was supported by JSPS KAKENHI Grant Number 20K14378 and JST CREST grant number JPMJCR18I2, Japan. The authors thank the Super-computer Center, the Institute for Solid State Physics, University of Tokyo for the use of the facilities. The simulations were also carried out using the facilities of the Research Institute for Information Technology, Kyushu University.

Received: ((will be filled in by the editorial staff))
Revised: ((will be filled in by the editorial staff))
Published online: ((will be filled in by the editorial staff))

References

[1] Y. Kudoh, H. Takeda, *Physica B & C* **1986**, *139*, 333.

[2] C. B. Agee, *Geophys. Res. Lett.* **1992**, *19*, 1169.

[3] W. E. Jackson, J. M. Deleon, G. E. Brown, G. A. Waychunas, S. D. Conradson, J. M. Combes, *Science* **1993**, *262*, 229.

[4] a) Q. Williams, E. Knittle, R. Reichlin, S. Martin, R. Jeanloz, *J. Geophys. Res.-Solid.* **1990**, *95*, 21549; b) G. Richard, P. Richet, *Geophys. Res. Lett.* **1990**, *17*, 2093.

[5] D. Andrault, M. A. Bouhifd, J. P. Itié, P. Richet, *Phys. Chem. Miner.* **1995**, *22*, 99.

[6] M. B. Kruger, R. Jeanloz, M. P. Pasternak, R. D. Taylor, B. S. Snyder, A. M. Stacy, S. R. Bohlen, *Science* **1992**, *255*, 703.

[7] a) X. F. Jiang, G. Y. Guo, *Phys. Rev. B* **2004**, *69*, 155108; b) L. Xiao, X. Li, X. Yang, *Eur. Phys. J. B* **2018**, *91*, 85.

[8] D. M. Ramo, L. Stixrude, *Geophys. Res. Lett.* **2014**, *41*, 4512.

[9] F. Shimojo, S. Fukushima, H. Kumazoe, M. Misawa, S. Ohmura, P. Rajak, K. Shimamura, L. Bassman, S. Tiwari, R. K. Kalia, A. Nakano, P. Vashishta, *SoftwareX* **2019**, *10*, 100307.

[10] a) P. E. Blochl, *Phys. Rev. B* **1994**, 50, 17953; b) G. Kresse, D. Joubert, *Phys. Rev. B* **1999**, *59*, 1758.

[11] J. P. Perdew, K. Burke, M. Ernzerhof, *Phys. Rev. Lett.* **1996**, *77*, 3865.

[12] V. I. Anisimov, F. Aryasetiawan, A. I. Lichtenstein, *J. Phys.-Condens. Matter* **1997**, *9*, 767.

[13] M. Misawa, S. Ohmura, F. Shimojo, *J. Phys. Soc. Jpn.* **2014**, *83*, 105002.

[14] M. Cococcioni, A. Dal Corso, S. de Gironcoli, *Phys. Rev. B* **2003**, *67*, 094106.

[15] M. Cococcioni, S. de Gironcoli, *Phys. Rev. B* **2005**, *71*, 035105.

[16] G. J. Martyna, M. E. Tuckerman, D. J. Tobias, M. L. Klein, *Mol. Phys.* **1996**, *87*, 1117.

[17] G. J. Martyna, D. J. Tobias, M. L. Klein, *J. Chem. Phys.* **1994**, *101*, 4177.

[18] J. S. Zhang, Y. Hu, H. Shelton, J. Kung, P. Dera, *Phys. Chem. Miner.* **2017**, *44*, 171.

[19] F. Béjina, M. Bystricky, N. Tercé, M. L. Whitaker, H. Chen, *C. R. Geosci.* **2019**, *351*, 86.

[20] S. Stackhouse, L. Stixrude, B. B. Karki, *Earth Planet. Sci. Lett.* **2010**, *289*, 449.

[21] E. Ryuo, D. Wakabayashi, A. Koura, F. Shimojo, *Phys. Rev. B* **2017**, *96*, 054206.

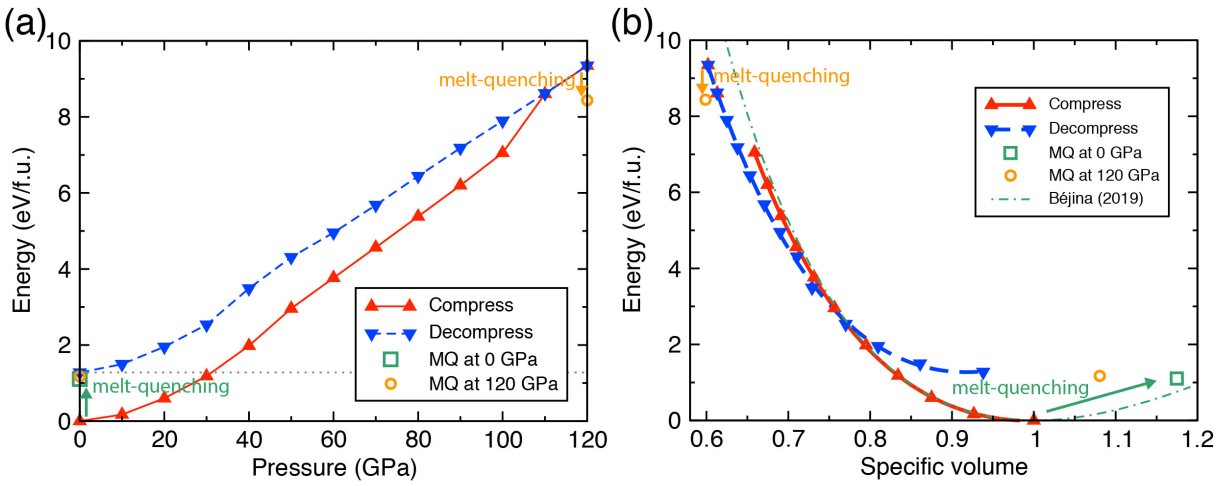

Figure 1. Average potential energy as a function of a) Pressure and b) average specific volume. The red and blue triangles indicate the compression and decompression processes, respectively. The solid and dashed lines in (a) were drawn by linear interpolation. The solid and dashed lines in (b) are fitting curves to the third-order BMEoS for the ranges 0-100 GPa and 120-0 GPa, respectively. The green squares and orange circles show the energetic properties of Fe_2SiO_4 glasses made by melt-quenching at 0 and 120 GPa, respectively. The green dashed dotted line in (b) indicates the energy and volume relation using elastic properties measured experimentally.[19]

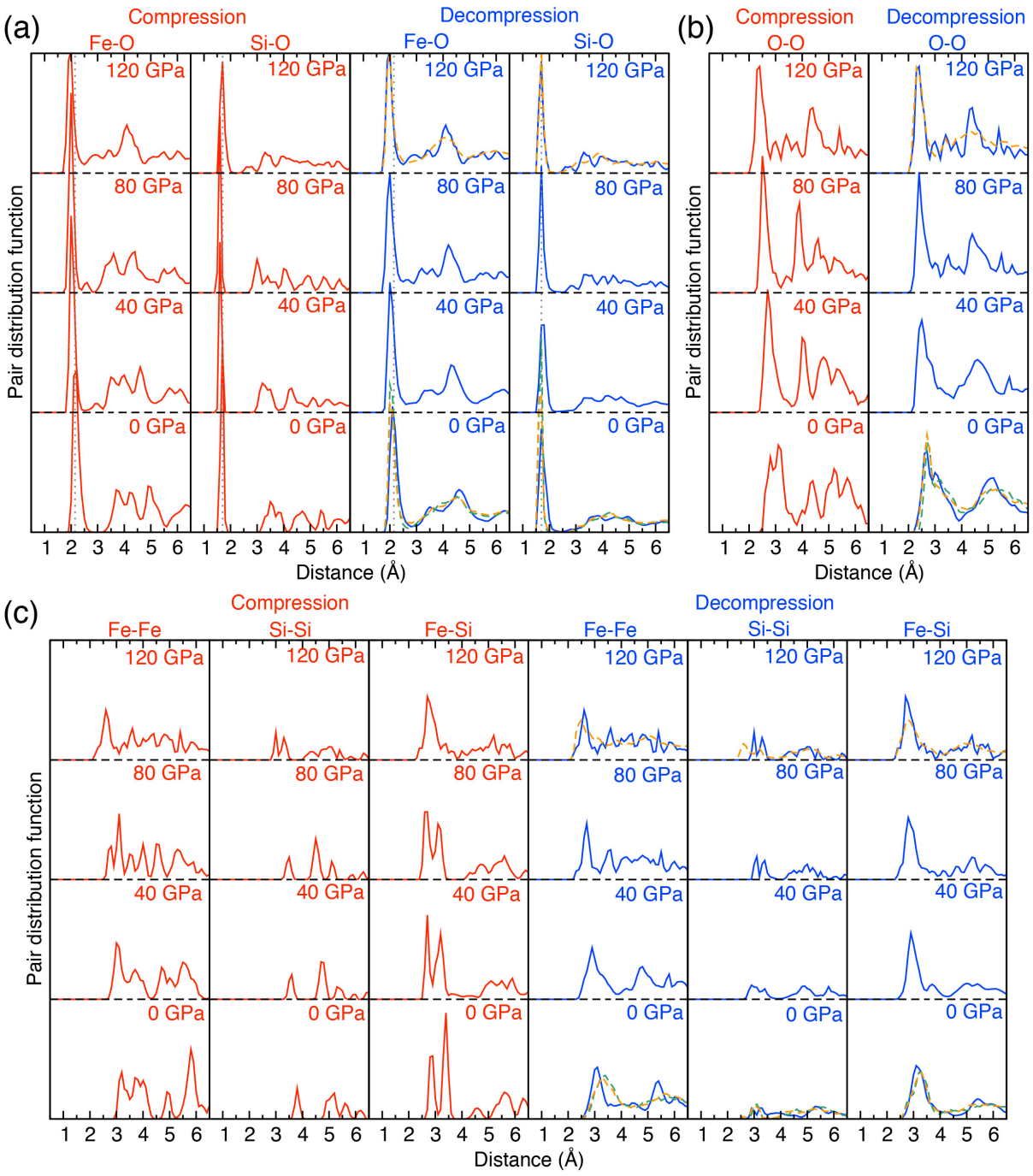

Figure 2. Pair distribution functions for a) cation-anion, b) anion-anion, and c) cation-cation pairs at 0, 50, 80 and 120 GPa. The red and blue solid curves correspond to the compression and decompression processes, respectively. The gray dotted lines in (a) indicate the main peak position of the crystalline phase at 0 GPa. The green and orange dashed curves correspond to the glasses made by melt-quenching at 0 and 120 GPa, respectively.

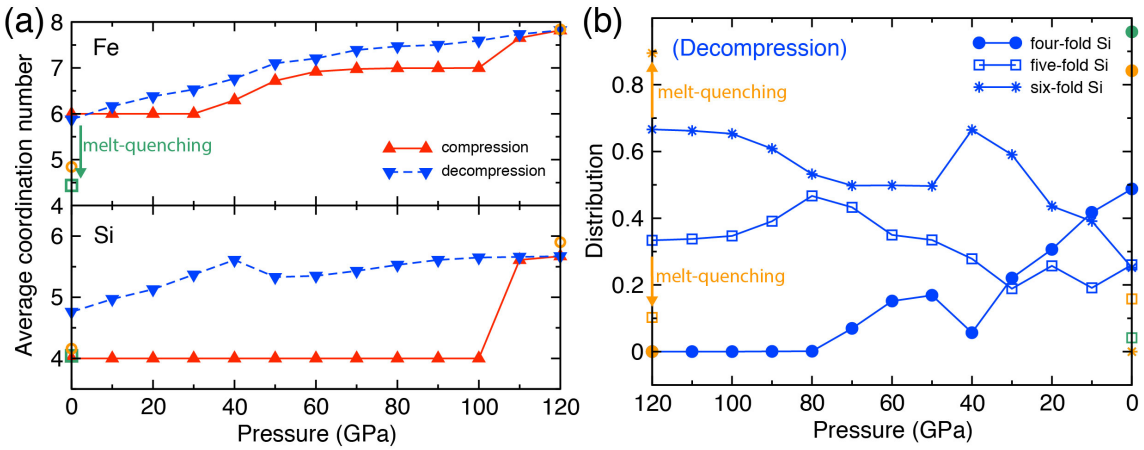

391

392 **Figure 3.** a) Average coordination numbers of Fe and Si atoms. The red triangles with a solid
393 line and blue triangles with a dashed line correspond to the compression and decompression
394 processes, respectively. b) Distribution of the coordination number of Si atoms as a function
395 of pressure. The filled circles, open squares and star symbols indicate the distributions of
396 four-fold, five-fold and six-fold coordinated Si atoms, respectively. The green and orange
397 symbols correspond to the glasses made by melt-quenching at 0 and 120 GPa, respectively.

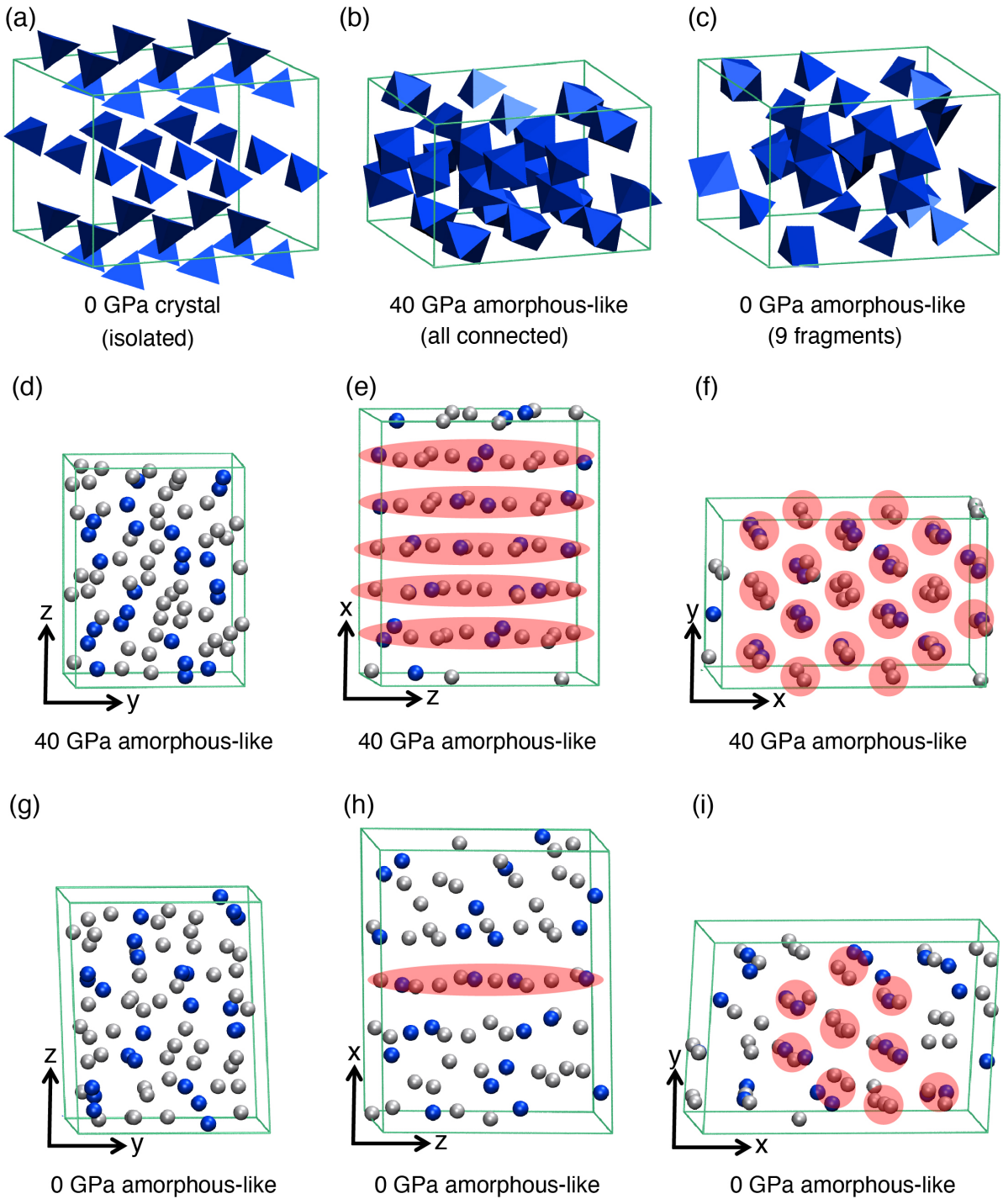

Figure 4. a-c) SiO_x polyhedrons in crystalline (a), amorphous-like at 40 GPa, and amorphous-like at 0 GPa (c). d-i) Fe and Si atoms in the amorphous-like phase at 40 GPa (d-f) and 0 GPa (g-i). The gray and blue spheres indicate Fe and Si, respectively. The green lines indicate the supercell edge.

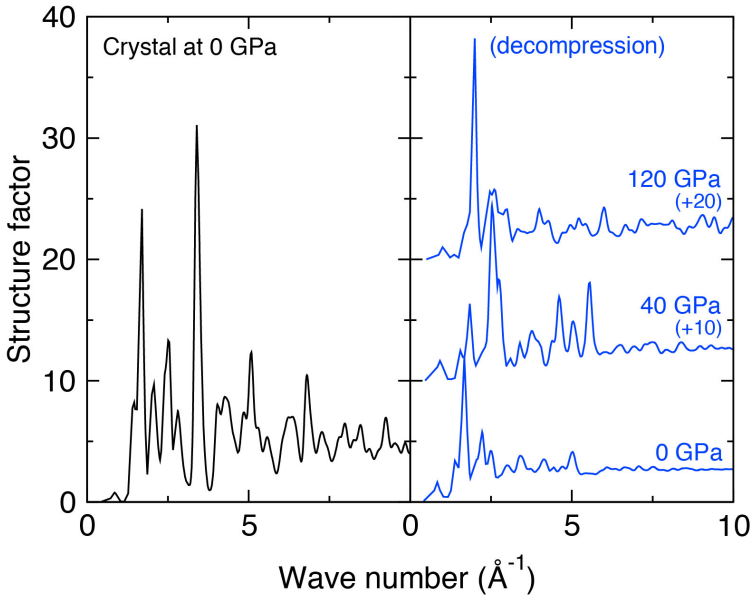

403

404 **Figure 5.** Structure factor of Crystal (left) and amorphous-like (right) phase.

405

406